

Recoverable Thermo-Responsive Polymeric Surfactants for the Synthesis of Bulk Plastics from Latexes

Nicolò Manfredini, Mattia Sponchioni,* and Davide Moscatelli

Cite This: *ACS Appl. Polym. Mater.* 2022, 4, 270–279

Read Online

ACCESS |



Metrics & More



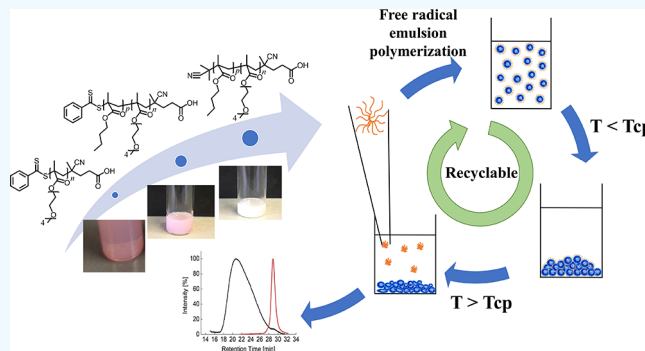
Article Recommendations



Supporting Information

ABSTRACT: Free-radical emulsion polymerization (eFRP) is widely adopted in industries due to the great advantages that this technique offers in terms of a high polymerization rate, good heat management, and conduction in a non-toxic solvent like water. On the other hand, eFRP requires surfactants to stabilize the produced polymer nanoparticles (NPs). At the same time, the recovery of a bulk material from a NP suspension needs the addition of salts or alkali for the destabilization of the emulsion and the precipitation of the polymer. These can contaminate the final product and affect its properties. For this reason, alternative strategies able to coagulate the NP latex avoiding the addition of exogenous compounds are needed. In this work, we synthesized thermo-responsive polymeric surfactants that are able to promote the NP formation during the eFRP and to allow the recovery of the bulk polymer by simply increasing the environment temperature. Surfactants with a tunable hydrophilic–lipophilic balance were produced through reversible-addition fragmentation chain transfer (RAFT) emulsion polymerization by chain-extending a polyethylene glycol-based macromolecular chain transfer agent with butyl methacrylate, in order to obtain a series of block copolymers with high blocking efficiency, controlled molecular weight distribution, and well-defined thermo-responsive behavior. Then, the RAFT agent was removed to avoid the further extension of the block copolymers, and the surfactants were tested in the eFRP of different monomers (i.e., butyl methacrylate, methyl methacrylate, and styrene) to produce stable NP latexes. Finally, the possibility of triggering the NP aggregation and of guaranteeing the recovery of both surfactants and bulk material by simply changing the temperature of the system was assessed.

KEYWORDS: surfactant, emulsion polymerization, hydrophilic–lipophilic balance, HLB, RAFT, CMC, thermo-responsive, temperature-induced aggregation



1. INTRODUCTION

With an annual production above 370 million tonnes,^{1–3} polymer materials are currently playing a leading role in a variety of everyday commodities, including synthetic rubbers, plastics, adhesives, paints, and coatings. Most of these products are processed and used as bulk materials. However, bulk polymerization faces many limitations, including the important increase in the product viscosity at high monomer conversion, which prevents an effective stirring of the reaction mixture and a difficult thermal control over the reactor, further exacerbated by the prevention of an effective heat exchange, bringing about the risk of thermal runaway.⁴

On the other hand, emulsion polymerization (eFRP) is a convenient route to produce nanostructured, high molecular weight polymers at a high polymerization rate using an environmentally friendly solvent.⁵ Because the polymerization is conducted inside nanoparticles (NPs) dispersed in a non-solvent, typically water, the viscosity is maintained low even at high conversion. In addition, the great advantage compared to a bulk process is represented by the water acting as a thermal

flywheel, thus enabling a more facile thermal control over the reactor. Despite these advantages in the conduction of the process, eFRP presents several drawbacks when a solid product is required. In particular, a bulk material can only be obtained following the latex coagulation. This can be achieved by water evaporation, which is often disregarded due to the high energy demand, or by precipitation following the addition of huge amounts of salt, acid, or alkali. Of course, this leads to the product contamination and to the production of high volumes of wastewater.

A milestone in the literature is the adoption of switchable stabilizers during the emulsion polymerization of vinyl monomers.⁶ The phase separation of these surfactants in

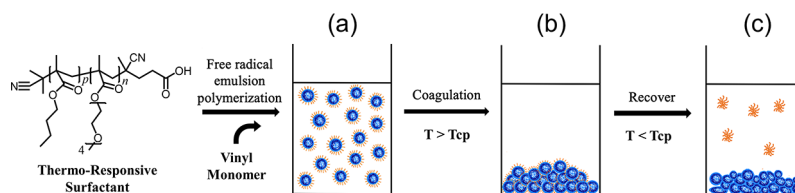
Received: September 23, 2021

Accepted: November 29, 2021

Published: December 13, 2021



Scheme 1. Schematic Representation of: (a) Production and (b) Coagulation of Polymer NPs When Thermo-Responsive Surfactants Are Used; (c) Recovery of the Surfactant as Micelles after Temperature Decrease



response to external stimuli allows producing reversibly dispersible and coagulatable latexes. Different stimuli have been investigated so far in the destabilization and redispersion of polymer colloids. In a series of papers, for example, the Zhu's group exploited the pH-reversible protonation/deprotonation of weak polyacids (i.e., polyacrylic acid⁷) or polyalkalis (i.e., poly[*N,N*-(dimethylamino)ethyl methacrylate]⁸) to turn on and off the stabilizing effect of macromolecular surfactants produced by reversible addition–fragmentation chain transfer (RAFT) polymerization. Other stimuli investigated so far include redox potential⁹ and above all CO₂/N₂ bubbling.^{10,11} Many of these approaches suffer the limitation that the surfactants are chemically linked to the polymer particles so that the produced material is contaminated by the surfactant itself.

In addition, to make this approach appealing on an industrial scale, the stimulus applied to destabilize the latexes should be inexpensive and easily operated and should prevent the contamination of water and hence the necessity for further treatments. A stimulus that meets these requirements is the application or removal of heat. Polymers that are able to respond to temperature modifications in the surrounding environment with a discontinuous and sharp phase transition are called thermo-responsive and are currently finding increasing interest for oil–water separation,^{12–14} chromatography,^{15,16} smart optics,^{17,18} and biomedical applications.^{19–23} Two opposite responses to temperature stimuli are reviewed, namely a lower critical solution temperature (LCST) behavior and an upper critical solution temperature (UCST) behavior.²⁴ The former is the minimum of the binodal curve that delimitates the region in the polymer/solvent phase diagram where separation in a polymer-rich phase occurs.^{25,26} At the opposite, the UCST is the maximum of the binodal curve delimitating the region where the polymer phase separates.^{27,28} Polymers with a LCST in water are the most common, mainly due to the poor sensitivity of this critical temperature to environmental properties such as pH, ionic strength or concentration, and the relative facility in tuning the cloud point (*T*_{cp}) in the desired range.²⁸

In this work, we report the synthesis of thermo-responsive polymeric surfactants with a LCST behavior. These switchable surfactants allow the production of stable polymer latexes below their *T*_{cp}, and their coagulation by temperature increase (Scheme 1a,b), without the addition of exogenous compounds (i.e., salts, alkali, CO₂, etc.) that may alter the properties of the produced material. The van der Waals forces between the coagulated particles prevent their redispersion upon cooling. At the opposite, the release of surfactant micelles at low temperature (Scheme 1c) paves the way for the surfactant reutilization in a further eFRP, in agreement with the recommendations of the circular economy. In fact, differently from other reported strategies, the surfactant is not covalently bound to the final polymer particles. This has the additional

advantage of avoiding the product contamination and the deterioration of its thermo-mechanical properties. It is worth mentioning that the choice of the *T*_{cp} is extremely important in designing these systems. In fact, it appears clear from the mechanism described above that the *T*_{cp} chosen should be sufficiently high to be compatible with the most commonly used thermal initiators since the eFRP can be conducted only at temperatures lower than *T*_{cp}. However, too high *T*_{cp}s are reflected in additional thermal energy required to lead to NP aggregation and polymer recovery. For these reasons, in order to address both these issues, surfactants with a *T*_{cp} in the range 60–70 °C have been selected as a good compromise. The thermo-responsive surfactants were synthesized *via* RAFT emulsion polymerization, by chain extending a poly[oligo-(ethylene glycol)methyl ether methacrylate] macromolecular chain transfer agent (macro CTA) with butyl methacrylate. The adoption of a controlled radical polymerization enabled us to control the molecular weight distribution of the copolymer and then the hydrophilic–lipophilic balance (HLB) of the surfactant. We have already reported in a previous study²⁹ the important role that this parameter plays, together with the NP concentration, in determining the stability and the size of the NPs and the reversibility of their thermo-responsive behavior. This information was used as a starting point to design thermo-responsive surfactants able to produce, in the following emulsion polymerization, stable and controlled NPs and to selectively mediate their precipitation avoiding the formation of a gel that would turn out in an inefficient polymer recovery.

The thermo-responsive surfactants were tested in the synthesis of stable NPs from various monomers, including butyl methacrylate, methyl methacrylate, and styrene. Finally, the possibility of inducing the NP coagulation and the surfactant recovery by changing the environment temperature was assessed.

2. MATERIALS AND METHODS

2.1. Materials. 2,2'-azobis(2-methylpropionamide)-dihydrochloride (V-50, MW = 271.19, 98%, Acros Organics), 2,2'-azobis(2-methylpropionitrile) (AIBN, MW = 164.21, ≥99%, Sigma-Aldrich), 4-cyano-4-(phenyl-carbonothioylthio)-pentanoic acid (CPA, MW = 279.38, 99%, Sigma-Aldrich), 4,4'-azobis(4-cyanovaleic acid) (ACVA, MW = 280.28, Sigma-Aldrich), acetone (≥99.5%, MW = 58.08, Honeywell), butyl methacrylate (BMA, ≥99%, MW = 142.20, Fluka Chemika), styrene (STY, ≥99%, MW = 104.15, Sigma-Aldrich), deuteriochloroform (CDCl₃, 99.8%, MW = 120.38, Sigma-Aldrich), dimethyl sulfoxide (DMSO, ≤0.02% water, MW = 78.13, Sigma-Aldrich), ethanol (EtoH, MW = 46.07, ≥99.8%, Sigma-Aldrich), hydrogen peroxide (H₂O₂, MW = 34.0147, 35%, Steris), methyl methacrylate (MMA, ≥99%, MW = 100.12, Fluka Chemika), pyrene (98%, MW = 202.25, Sigma-Aldrich), poly(ethylene glycol)methyl ether methacrylate (EG₄MA, MW = ca300, Sigma-Aldrich), and tetrahy-

Table 1. List of All the Polymers Synthesized with Their Properties, Where n and p Are the Degrees of Polymerization Calculated from ^1H NMR for the Poly(EG_4MA) and the Poly(BMA) Blocks, Respectively^a

entry	sample	HLB [-]	$n_{\text{H NMR}}$ [-]	$p_{\text{H NMR}}$ [-]	M_{GPC} [Da]	D_{GPC} [-]	$X_{\text{H NMR}}$ [%]	CMC [mg/L]
1	20EG ₄	20	23		6900	1.04	97	
2	40EG ₄	20	49		11,400	1.02	94	
3	20EG ₄ -32BMA	13	23	37	8000	1.09	98	5.73 ± 0.31
4	20EG ₄ -48BMA	11	23	50	7100	1.05	94	5.01 ± 0.40
5	20EG ₄ -72BMA	9	23	71	10,700	1.12	97	2.44 ± 0.32
6	20EG ₄ -110BMA	7	23	107	20,700	1.03	95	0.31 ± 0.35
7	20EG ₄ -176BMA	5	23	170	57,400	1.03	93	0.49 ± 0.11
8	40EG ₄ -40BMA	13	49	40	12,900	1.07	96	8.76 ± 0.71
9	40EG ₄ -66BMA	11	49	70	12,300	1.06	99	8.63 ± 0.23
10	40EG ₄ -100BMA	9	49	103	14,900	1.06	94	1.27 ± 0.12
11	40EG ₄ -150BMA	7	49	148	37,200	1.01	96	0.14 ± 0.54
12	40EG ₄ -229BMA	5	49	231	45,200	1.09	97	0.26 ± 0.09
13	40EG ₄ -522BMA	3	49	530	50,600	1.01	97	0.12 ± 0.08
14	40EG ₄ -1000BMA	1.5	49	980	83,800	1.22	98	0.11 ± 0.06
15	40EG ₄ -3000BMA	0.5	49	2970	102,500	1.08	99	0.09 ± 0.06

^a M_{GPC} represents the number-average molecular weight, D represents the dispersity, $X_{\text{H NMR}}$ represents the conversion calculated via ^1H NMR, and CMC represents the critical micelle concentration determined via the fluorescent method using pyrene as the probe.

dofuran (THF, ≥99.9%, MW = 72.11, Sigma-Aldrich) were used as received except when specifically noted. All the solvents used were of analytical purity and used as received.

2.2. Synthesis of the Thermo-Responsive Block. The thermo-responsive portions of the surfactant were synthesized via RAFT polymerization of EG_4MA with CPA as the RAFT agent, ACVA as initiator, and ethanol as solvent. The average degree of polymerization (n) was varied by changing the monomer to CPA molar ratio in order to obtain two different stabilizers with n equal to 20 and 40, respectively. The initiator to the agent RAFT molar ratio (IA) was kept equal to 1/3. The solution mass concentration was set equal to 20%.

As an example, to synthesize the macro CTA with $n = 40$, hereinafter 40EG₄, 10 g of EG_4MA (33 mmol), 0.232 g of the RAFT agent (0.83 mmol, *i.e.*, $\text{EG}_4\text{MA}/\text{RAFT agent} = 40$ mol/mol), and 0.078 g of ACVA (0.28 mmol, *i.e.*, IA = 1/3 mol/mol) were dissolved in 41 g of ethanol and poured in a round-bottom flask equipped with a magnetic stirrer. The solution was purged with nitrogen for 20 min at room temperature and heated to 65 °C in an oil bath under magnetic stirring for 24 h. At the end of the polymerization, the product was recovered by precipitation in 10-fold excess diethyl ether, performed twice. Finally, the suspension was centrifuged at 5000 rpm for 10 min, and the polymer was recovered, dried under a flow of nitrogen, and stored at -20 °C. In order to calculate the conversion (eq S1), 10 mg of polymer was dissolved in 0.7 mL of deuterated chloroform (CDCl_3) and analyzed via nuclear magnetic resonance (^1H NMR) (spectrum in Figure S1) on a Bruker Ultrashield 400 MHz spectrometer with 32 scans per sample.

The number-average molecular weight (M_{GPC}) and dispersity (D) were evaluated via organic gel permeation chromatography dissolving 4 mg/mL polymer in THF, filtering the solution through a 0.45 μm polytetrafluoroethylene filter, and injecting it in a Jasco LC-2000Plus GPC apparatus. The analysis was performed at 35 °C and at a flow rate of 1 mL/min using three styrene/divinyl benzene 5 μm columns in series (300 × 8 mm, pore size 1000, 10⁵, and 10⁶ Å, respectively) and a pre-column (50 × 8 mm). Polystyrene standards were used to calibrate the instrument.

2.3. Synthesis of the Thermo-Responsive Surfactants via RAFT Emulsion Polymerization. The chain extension of the two different macro CTAs (with $n = 20$ and 40) with butyl methacrylate was carried out via RAFT emulsion polymerization. In this reaction, V-50 was used as initiator. $n\text{EG}_4$ - $p\text{BMA}$ block copolymers with different HLB were synthesized by modulating p , with p being the degree of polymerization of the poly(butyl methacrylate) segment. In particular, the HLB was calculated according to Griffin's method (eq 1).³⁰

$$\text{HLB} = 20 \frac{M_{\text{h}}}{M} \quad (1)$$

Where M_{h} is the molar mass of the hydrophilic portion of the surfactant, while M is the molar mass of the surfactant. The desired HLB can be obtained at fixed M_{h} by changing M through the modulation of p . With this approach, we synthesized 40EG₄- $p\text{BMA}$ surfactants with the HLB equal to 0.5, 1.5, 3, 5, 7, 9, 11, and 13 and 20EG₄- $p\text{BMA}$ surfactants with the HLB equal to 5, 7, 9, 11, and 13.

For all the reactions, the initiator to the macro CTA molar ratio was set to 1/3, and the solid content was equal to 10% w/w. As an example, the 40EG₄-100BMA (*i.e.*, theoretical HLB = 11) surfactant was synthesized by mixing 0.225 g of BMA (1.6 mmol), 0.275 g of 40EG₄ (0.016 mmol, *i.e.*, $\text{BMA}/40\text{EG}_4 = 100$ mol/mol), and 1.4 mg of V-50 (5.6 μmol, *i.e.*, $\text{V-50}/40\text{EG}_4 = 1/3$ mol/mol) in 4.5 g of distilled water. The reaction was carried out in 10 mL round-bottom flasks equipped with a magnetic stirrer operated at 600 rpm. The mixture was purged for 15 min by bubbling nitrogen inside the reaction environment to remove all the oxygen and was then placed in an oil bath pre-heated at 50 °C for 24 h. The product was finally dialyzed against distilled water for 48 h using a regenerated cellulose membrane (Spectra/Por) with a molecular weight cut-off of 3.5 kDa.

An aliquot of the sample was freeze-dried using a Telstar Lyoquest freeze-dryer operated at -56 °C and 0.1 mbar and analyzed by GPC according to the procedure described in Section 2.2. The molecular weights and dispersities of the samples are listed in Table 1. The monomer conversion was evaluated both via ^1H NMR (Figure S2), according to the procedure described in Section 2.2, and via thermogravimetric

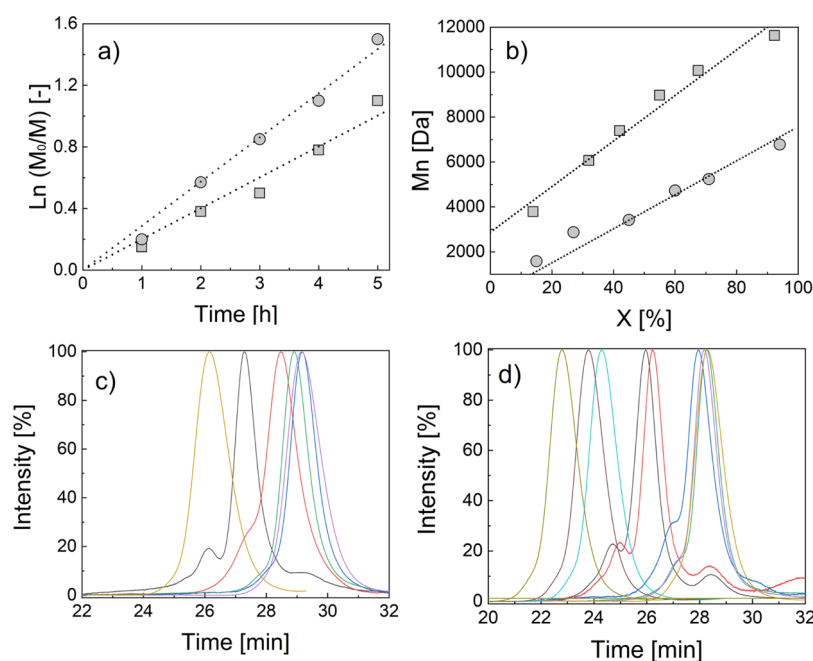


Figure 1. (a) $\ln(M_0/M)$ as a function of time in the case of 40EG₄ (squares) and 20EG₄ (circles). (b) Number-average molecular weight as a function of the monomer conversion in the case of 40EG₄ (squares) and 20EG₄ (circles). (c) Chromatograms of the polymers synthesized from 20EG₄ having the HLB equal to 5 (yellow), 7 (black), 9 (red), 11 (green), 13 (purple), and 20 (blue), respectively. (d) Chromatograms of the polymers synthesized from 40EG₄ having the HLB equal to 0.5 (dark yellow), 1.5 (burgundy), 3 (azure blue), 5 (black), 7 (red), 9 (blue), 11 (purple), 13 (green), and 20 (yellow), respectively.

analysis performed on an Ohaus MB35 moisture analyzer according to the procedure reported in a previous work.³¹

The micelle suspensions were analyzed *via* dynamic light scattering (DLS) in order to determine the T_{cp} , particle size (D_n), and polydispersity index (PDI). The measurements were performed in triplicate, 11 runs each, on a Zetasizer Nano ZS at a scattering angle of 173°. The samples were diluted to 0.5% w/w before the analysis. The T_{cp} was determined as the inflection points of D_n versus temperature curves. These curves were obtained by increasing/decreasing the temperature by 2 °C and leaving the sample to equilibrate at that specific temperature for 10 min before each measurement.

2.4. Determination of the CMC. The critical micellar concentration (CMC) of the nEG_4 -*p*BMA polymers was evaluated via fluorometric analysis using pyrene as a hydrophobic fluorescent probe.

In particular, a pre-determined amount of pyrene was dissolved in acetone, placed into different vials, and put on a heating plate in order to allow the evaporation of acetone. Then, 5 mL of polymer suspensions at different concentrations (0.01, 0.05, 0.1, 0.5, 1, 5, 10, 50, and 100 mg/L) were added in order to have a final concentration of pyrene equal to 6×10^{-7} M (4.854×10^{-7} g per vial). The vials were vortex-stirred for 1 min and placed in a closed box for one night. Pyrene emission spectra were then recorded on a Jasco FP8500 spectrofluorometer setting the excitation wavelength to 335 nm and the emission wavelength in a range from 350 to 450 nm. Excitation and emission band widths were set at 5 and 2.5 nm, respectively.

The intensity ratio of the third band (i.e., 384 nm, I_3) to the first band (i.e., 373 nm, I_1) was analyzed in order to determine the CMC as a function of the polymer concentration. In particular, the CMC was considered as the intersection between the horizontal asymptote of I_3/I_1 at a low

concentration and the logarithmic function of I_3/I_1 with the polymer at a high concentration.^{19,32}

2.5. Removal of the Thiocarbonylthio Group through the Addition of AIBN. The removal of the thiocarbonylthio group from the chain end of each polymeric surfactant, important to avoid its chemical incorporation in the forming polymer NPs, was achieved through the addition of a 100 mg/mL solution of AIBN in DMSO.

The reactions were carried out in 10 mL round-bottom flasks equipped with magnetic stirrers.

The AIBN to nEG_4 -*p*BMA was set equal to 40 mol/mol. In order to remove all the oxygen from the flasks, the mixtures were purged for 15 min by bubbling nitrogen inside the reaction environment. Then, the flasks were placed in an oil bath pre-heated at 50 °C under magnetic stirring, and the reaction was carried out for 12 h. At the end of the reaction, ¹H NMR measurements were performed following the same procedure described in Section 2.2.

Finally, the D_n of the micelles was analyzed via DLS.

2.6. Emulsion polymerization Using nEG_4 -*p*BMA Surfactants. nEG_4 -*p*BMA polymers were used as surfactants for the eFRP of butyl methacrylate, methyl methacrylate, and styrene. For all the reactions, the initiator was V-50. The initiator amount was set equal to 1.5% w/w with respect to the monomer, and the surfactant to monomer weight ratio was equal to 10% w/w, and the solid content was equal to 10% w/w.

As an example, 1 g of BMA, 0.1 g of 40EG₄-100BMA, and 15 mg of V-50 were mixed in 9 g of distilled water. The reaction was carried out in a 10 mL round-bottom flask equipped with a magnetic stirrer. The oxygen from the flasks was removed by bubbling nitrogen for 15 min inside the reaction environment. The flasks were placed in an oil bath pre-heated to 50 °C

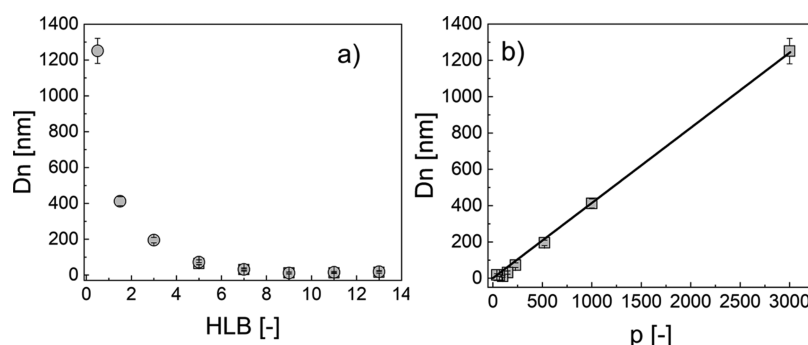


Figure 2. (a) Dn as a function of the HLB for both 20EG₄- (square) and 40EG₄-based micelles (circle). (b) Dn as a function of the degree of polymerization p of the lipophilic block for the 40EG₄-based micelles.

under magnetic stirring at 900 rpm, and the polymerization was carried out for 24 h.

The conversion was evaluated via thermogravimetric analysis according to the procedure described in Section 2.3. The NP size and PDI were characterized by DLS. Finally, the temperature-mediated NP coagulation was obtained by incubating the suspension at 80 °C for 30 min. After the polymer precipitation, the temperature was lowered to 25 °C to favor the surfactant desorption and migration in the aqueous phase. The bulk polymer obtained after precipitation was then recovered by filtration, dried under a flow of nitrogen, and characterized in terms of molecular weight *via* GPC, following the same procedure reported in Section 2.2.

3. RESULTS AND DISCUSSION

3.1. Thermo-Responsive Polymeric Surfactants. Thermo-responsive surfactants, in the form of amphiphilic block copolymers, were synthesized by chain extending PEG-based macro CTAs with BMA *via* RAFT emulsion polymerization.

First, we synthesized *via* RAFT solution polymerization the thermo-responsive portions of the surfactants, namely 20EG₄ and 40EG₄, reported with an LCST of approximately 64 °C.^{19,33} The good control of the RAFT polymerization over the process is confirmed by the low polymer dispersities \bar{D} (<1.04, Table 1) and by the linear evolution of $\ln(M_0/M)$ with time, as shown in Figure 1a. This is typical for those pseudo-living polymerizations characterized by a constant radical concentration in the system. In addition, the number-average molecular weight M_n grows linearly with the monomer conversion (Figure 1b), as expected from eq 2, valid for the RAFT polymerization under the assumption of negligible amount of initiator compared to the chain transfer agent.³⁴

$$M_n = M_{\text{CPA}} + nXM_{\text{EG}_4\text{MA}} \quad (2)$$

Where M_n is the polymer number-average molecular weight, n is the degree of polymerization that coincides with the molar ratio between the monomer and CTA, X is the monomer conversion, and M_{CPA} and $M_{\text{EG}_4\text{MA}}$ are the molecular weights of the CPA and EG₄MA, respectively.

These thermo-responsive macro CTAs were then chain-extended with BMA *via* RAFT emulsion polymerization to obtain amphiphilic block copolymers. For each macro CTA, different lengths p of the hydrophobic segment were targeted. The target p for this lipophilic block was determined a priori by fixing the desired HLB, which was calculated with Griffin's method (eq 1).³⁰ In fact, the adoption of a controlled radical polymerization like the RAFT polymerization enables the

expression of both M_n and M in eq 1 as a function of n and p , respectively, according to eq 3, derived under the hypothesis of complete monomer conversion.

$$\text{HLB} = 20 \frac{M_{\text{CPA}} + nM_{\text{EG}_4\text{MA}}}{M_{\text{CPA}} + nM_{\text{EG}_4\text{MA}} + pM_{\text{BMA}}} \quad (3)$$

Where M_{CPA} , $M_{\text{EG}_4\text{MA}}$, and M_{BMA} are the molecular weights of the CPA, EG₄MA, and BMA, respectively. Once the macro CTA is selected, and hence n is fixed, it is possible to determine the required p for achieving the desired HLB.

The adoption of the RAFT polymerization is crucial at this stage, since it enables the achievement of good control over the polymer microstructure and the access to well-defined block copolymers with high monomer conversion ($X > 94\%$, Table 1), low dispersities ($\bar{D} < 1.22$), and high blocking efficiencies, as observed from the chromatograms reported in Figure 1c,d.

Furthermore, since the polymers are produced *via* RAFT emulsion polymerization, the polymeric surfactants are expected to be obtained in the form of micelles. As a matter of fact, we obtained micelles whose size (Dn) depends on the HLB of the polymeric surfactant. In particular, the lower the HLB the bigger the micelles, as shown in Figure 2a. Moreover, it is possible to distinguish between a plateau region and an exponential region depending on whether the hydrophobic or hydrophilic contribution is predominant (i.e., the HLB is lower or higher than 9). Interestingly, the threshold HLB delimitating the two regions is the same for both the macro CTAs used (20 and 40EG₄).

The trend in the exponential region is due to the contribution of the progressively growing lipophilic block, determining a linear increase in the micelle size with p , as clearly shown in Figure 2b. This trend is in accordance with that already reported in the literature for similar systems and summarized in eq 4.³⁵

$$D_n = \frac{6pM_{\text{BMA}}}{A_{\text{cov}}N_{\text{avo}}\rho_{\text{pBMA}}} \quad (4)$$

Where N_{avo} is the Avogadro number, ρ_{pBMA} is the density of the lipophilic segment of the copolymer, and A_{cov} is the surface of the micelle that the hydrophilic portion can cover, which in this case is directly related to its length n .

Conversely, when the hydrophilic contribution became more important (HLB higher than 9), the further reduction in Dn is probably counter-balanced by the micelle swelling.

Despite the broad difference in size, narrowly dispersed particles were achieved in all of the cases (see Table S1). In

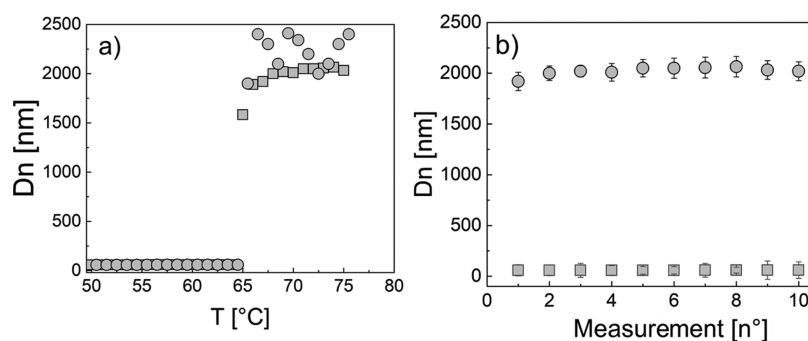


Figure 3. (a) D_n as a function of temperature for 40EG₄-229BMA during heating (squares) and cooling (circles) cycles. The analysis was conducted by DLS with a temperature increase/decrease of 2 °C per each measurement and leaving 10 min of equilibration at each temperature before the analysis. (b) D_n below (squares) and above (circles) the T_{cp} in the case of 40EG₄-229BMA.

addition, p does not affect appreciably the cloud point of the system. In particular, all of the samples show a sharp phase separation at 64 °C (Table S1), leading to the reversible formation of micrometric aggregates with a very limited hysteresis in the heating and cooling behavior. This is clearly shown in the example reported in Figure 3a by the sharp change in the NP size occurring at the same temperature (*i.e.*, 64 °C) in the heating (squares) and cooling (circles) cycles. This behavior is due to the fact that the micelles are sterically stabilized by their thermo-responsive segments, which above the T_{cp} collapse on the micelle surface. In this scenario, the van der Waals interactions are no longer balanced by the steric repulsion forces between the EG₄ chains, thus causing the micelle coagulation. Nevertheless, once the temperature is lowered back below the T_{cp} , the EG₄ chains extend in the bulk, thus re-stabilizing the micelles that recover their original size (see the circles in Figure 3a). This reversibility is impacted by the block copolymer microstructure that needs to be carefully designed in order to allow the NP redispersion.²⁹

These sharp transitions, fundamental to guarantee a rapid and efficient coagulation of the polymer NPs produced during the successive eFRP (Scheme 1b), underline the homogeneity of the micelle response to the external stimuli.

The reversibility of these systems was proved to be maintained for at least 10 heating/cooling cycles, as shown in Figure 3b. This result is particularly important for the final application of these materials because it allows several recycles of the same polymer, thus reducing both production and process costs.

Finally, the possibility of using these systems as surface active agents was assessed by evaluating their CMC, a distinctive feature of the surfactant molecules. In particular, the CMC was determined according to the procedure described in Section 2.4. As can be retrieved from Table 1 and Figure 4, all of the polymers synthesized showed a CMC, confirming their ability of forming micelles and hence of being effectively used as surfactants. Moreover, the values of the CMC, considerably lower than those of the commercial surfactants (*e.g.*, SDS, CMC = 2.45 g/L³⁶), pave the way for the employment of these materials on an industrial scale without any particular change in the synthesis recipes.

Interestingly, the CMC resulted to be, after an initial plateau, a linear function of the HLB. This is not surprising, and in fact, polymeric surfactants with a high HLB are more hydrophilic and hence characterized by more thermodynamically stable polymer–water interactions that make them less prone to assemble and form micelles. This can justify also the higher

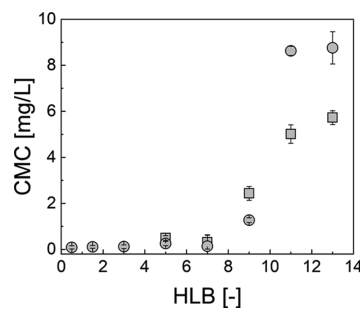


Figure 4. CMC as a function of the HLB for surfactants synthesized employing 20EG₄ (squares, entries 3–7 in Table 1) and 40EG₄ (circles, entries 8–15 in Table 1) as a macro CTA, respectively.

CMC that the 40EG₄-based surfactants have with respect to that of the 20EG₄-based ones.

Once the possibility of producing polymeric surfactants with a tunable HLB and defined values of the CMC is demonstrated, an important step is the removal of the thiocarbonylthio group from the polymer chain end. This is necessary in order to avoid the chemical incorporation of the surfactant in the polymer NPs produced in the following eFRP (Scheme 1). This is a key point for the sustainability of the process because it prevents the contamination of the polymers produced and at the same time allows the recovery and recycle of the surfactants.

In fact, in the case in which the RAFT agent is not removed, the polymerization proceeds via chain extension of the lipophilic block producing multiblock copolymers and preventing its separation from the latex once the temperature is increased (Figure 5a). On the contrary, when the RAFT agent is removed, the new monomer and initiator added to the mixture can polymerize following the same rules as those of a traditional eFRP, while the macro-surfactants act as stabilizers (Figure 5b).

The removal of the thiocarbonylthio group was carried out with an excess of AIBN. The effective removal of the RAFT agent can be easily seen visually. In fact, as soon as the thiocarbonylthio group is removed, the polymeric suspension changes its color from pink to white. However, the confirmation of the success of the reaction was obtained noticing the disappearance of the peaks associated to the aromatic ring in the ¹H NMR spectrum of the polymers reacted with AIBN, as shown in Figure 5c.

Moreover, the reaction with AIBN does not modify the D_n and the CMC of the macro-surfactants, as visible in Table S2.

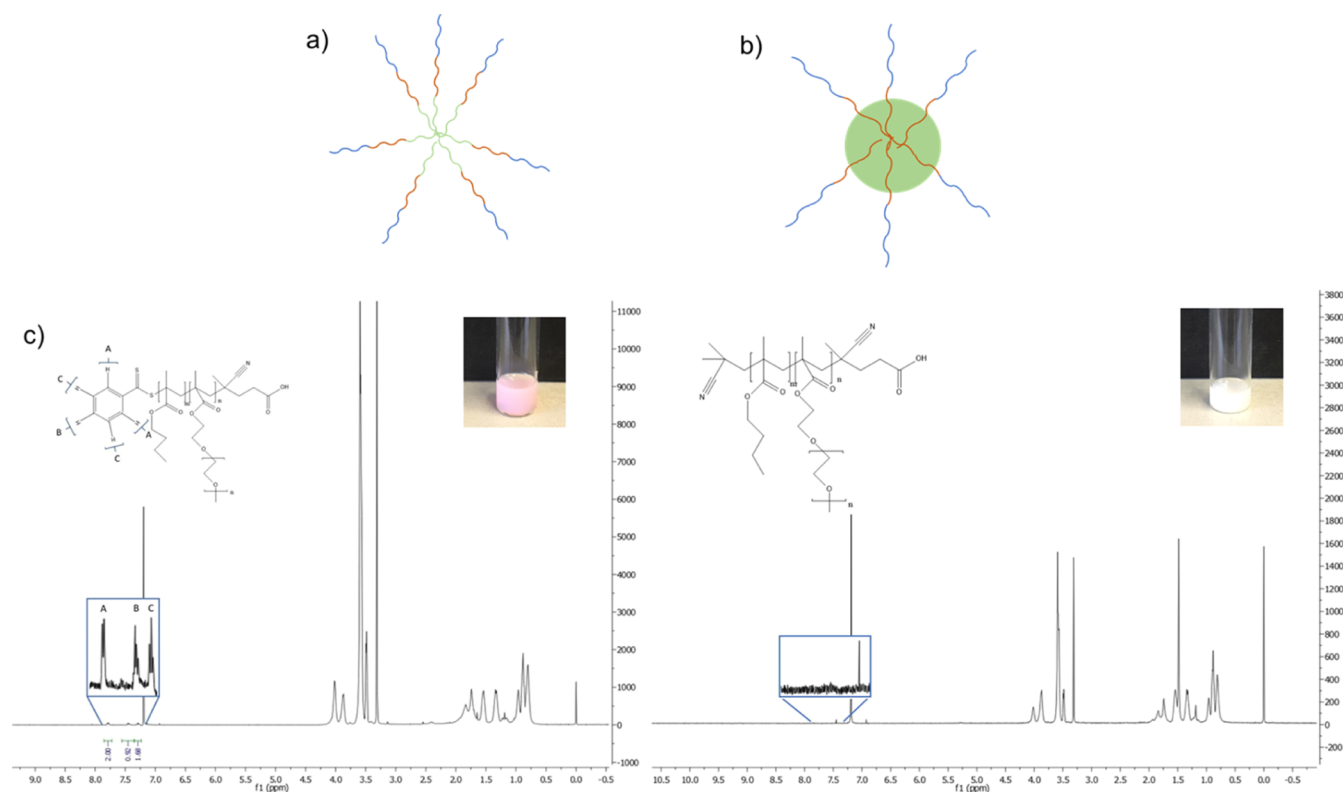


Figure 5. Emulsion polymerization in case the RAFT agent is still present (a) or has been removed (b). (c) Surfactant $^1\text{H-NMR}$ spectrum before (left) and after (right) the removal of the RAFT agent with AIBN. The complete removal of the thiocarbonylthio group is testified by the disappearance of the signal originating from the aromatic ring in the CPA, in the region 7–8 ppm, and by the change of the micelle color, from pink to white, as shown in the inset.

Because during the eFRP, the stabilizers may be subjected to variations of pH, we tested their stability, by measuring the average size and polydispersity of the micelles formed by the thermo-responsive surfactants in diluted HCl and NaOH solutions, at pH = 3 and 11, respectively. As shown in Table S3, these parameters are only poorly affected by the pH, with random fluctuations around the values assumed in a neutral environment. At the same time, these fluctuations are within the experimental error, which allows us to conclude that the behavior of these surfactants is stable in the range of investigated pH.

3.3. Free-Radical Emulsion Polymerization with Thermo-Responsive Surfactants. In order to verify the effective capability of these surfactants to allow both the production of stable polymer NPs and their coagulation via thermal stimulation, we first explored the eFRP of butyl methacrylate.

As shown in Table S4, all of the thermo-responsive surfactants allowed the production of NPs with narrow particle size distribution, in line with what is normally obtained performing an eFRP with commercial surfactants. Moreover, surfactants with a different HLB resulted in NPs with a different size, as clearly visible in Figure 6a. In particular, for both 40EG₄- and 20EG₄-based surfactants, smaller NPs can be achieved at a high HLB. This testifies that the size of the micelles formed by the surfactants, decreasing with the HLB, contributes to the final hydrodynamic diameter of the colloids produced.

The latexes produced proved to be stable until the temperature is kept below the T_{cp} of the surfactant. In fact, when the latex is incubated at a temperature above the T_{cp},

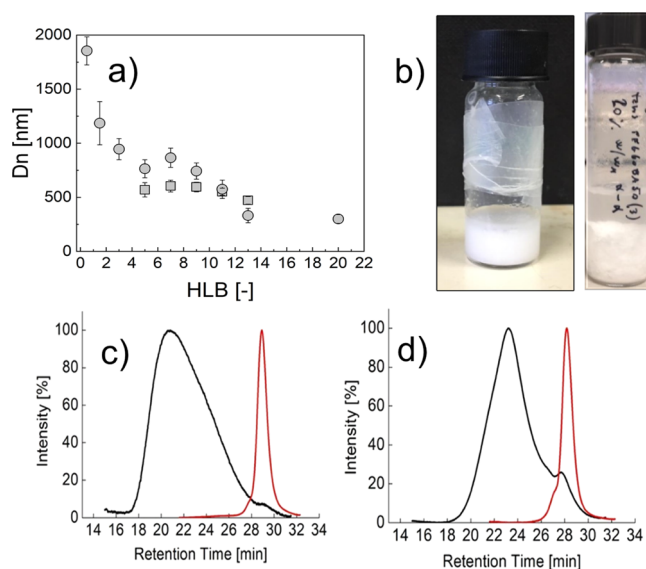


Figure 6. (a) Dn of the butyl methacrylate NPs synthesized via eFRP as a function of the HLB of the thermo-responsive surfactants. (b) NPs before (left) and after (right) thermal stimulation above the T_{cp}. (c) Normalized chromatograms of the polymer recovered from the eFRP using 20EG₄-32BMA as a surfactant (black) and of the same surfactant before the emulsion polymerization (red). (d) Normalized chromatograms of the polymer recovered from the eFRP using 40EG₄-40BMA as a surfactant (black) and of the same surfactant before the emulsion polymerization (red).

the NPs start to aggregate as it can be inferred from the high size and the broad dispersity reached, as reported in Table S4.

At the same time, once the temperature is decreased again below the T_{cp} , the surfactant molecules tend to migrate in water, while the bulk polymer remained at the bottom of the vial, as visible in Figure 6b, thus allowing its recovery. In fact, the detached surfactant molecules form again micelles with a size comparable to the one before the eFRP, as shown in Table 2. This suggests that the RAFT agent was properly removed

Table 2. Mn and Dispersity of the Polymer Produced via eFRP; Dn and PDI of the Recovered Surfactant Micelles

surfactant	$M_{n, GPC}$ [Da]	D_{GPC} [-]	D_n [nm]	PDI [-]
20EG ₄ -32BMA	353,900	1.45	17	0.15
20EG ₄ -48BMA	296,700	1.78	12	0.01
20EG ₄ -72BMA	157,800	1.53	13	0.12
20EG ₄ -110BMA	143,700	1.65	32	0.14
20EG ₄ -176BMA	125,800	1.77	65	0.15
40EG ₄ -40BMA	79,300	2.46	21	0.11
40EG ₄ -66BMA	287,800	1.97	13	0.12
40EG ₄ -100BMA	111,400	1.93	10	0.09
40EG ₄ -150BMA	89,200	1.86	35	0.08
40EG ₄ -229BMA	160,300	1.42	76	0.12
40EG ₄ -522BMA	135,800	1.87	201	0.13
40EG ₄ -1000BMA	178,500	1.67	408	0.11
40EG ₄ -3000BMA	198,300	2.12	1240	0.08

and that the surfactants were not chemically incorporated in the polymer chains. This evidence is further supported by the molecular weight distribution of the polymer recovered after the coagulation, as reported in Figure 6c,d. In fact, the residual surfactant that could not be resuspended after lowering the temperature generates a small shoulder in the chromatogram at approximately 29 min (black curve). To confirm that this actually corresponds to the surfactant, its chromatogram before the eFRP has been superimposed as a red curve. The molecular weight distributions of the produced polymer and the surfactants are clearly distinguished, which confirms that the surfactant was not incorporated in the product. If the opposite was true, the surfactant would have been chain-extended by the new monomer, producing a unique polymer and therefore a single peak in the chromatogram.

These surfactants proved to be versatile, allowing the production of narrowly distributed NPs also when methyl methacrylate and styrene were used as monomers in the eFRP, as can be seen from Table S5. These results confirm the suitability of these thermo-responsive surfactants in the production and easy recovery of high molecular weight polymers.

Finally, even if the price of these surfactants is higher than that of the traditional ones, the possibility of re-using these polymers more than once coupled with the possibility of directly recovering the bulk material without contamination (*i.e.*, addition of aggregating molecules) paves the way for the possible commercialization of these systems. To prove the reutilization of the surfactants, the sample 20EG₄-32BMA was reprocessed over 3 consecutive recovery/reutilization cycles. The results in terms of molecular weight distribution and surfactant recovery efficiency are reported in Table 3.

High molecular weight poly(butyl methacrylate) could be produced in all of the cycles using the same surfactant without reintegration. A peculiarity is represented by the recovery higher than 100% in the first two cycles. This was attributed to the redispersion of polymer fines when the temperature was

Table 3. Mn and Dispersity of the Polymer Produced via eFRP over Three Consecutive Surfactant Recovery and Reutilization Cycles, Each Characterized by a Specific Recovery

cycle no.	$M_{n, GPC}$ [Da]	D_{GPC} [-]	surfactant recovery [%]
1	353,900	1.45	116
2	492,000	1.81	109
3	477,600	2.10	88

lowered below the T_{cp} to recover the surfactant micelles. However, this is not necessarily a drawback, since the polymer dispersed in the aqueous phase can be exploited as a seed during the following eFRP, as it is typically done in industrial polymer production. The seeded eFRP that was actually performed during cycles 2 and 3 might also be responsible for the significant increase in the average molecular weight of the produced polymer, significantly different from the one produced during the first cycle when a fresh surfactant was used. As a matter of fact, despite being significantly different from the value measured after the first cycle, the M_n and D measured for cycles 2 and 3 are quite comparable, within the experimental variability.

Overall, we demonstrated that the reversible surfactants reported in this work can be recovered and reutilized up to three times, thus contributing to the sustainability of the process.

4. CONCLUSIONS

In this work, we developed a new class of thermo-responsive surfactants for the production of high molecular weight polymers via eFRP.

The use of a controlled and pseudo-living polymerization technique was fundamental to produce surfactants in the form of block copolymers with a high blocking efficiency and controlled HLB. In particular, the first parameter resulted to be extremely important in the obtainment of surfactants able to homogeneously and rapidly answer to an external stimulus. On the other hand, the HLB resulted to be a key parameter that allowed to tune the CMC of the surfactants, the size of the micelles formed above the CMC, and the particle size distribution of the final latexes.

The peculiarity of the produced surfactants is their sensitivity to temperature stimuli. In fact, the polymer micelles are stable and can stabilize polymer NPs as long as the temperature is below the T_{cp} , while collapse leading to the aggregation of the polymer NPs following the phase separation of the thermo-responsive block above the T_{cp} . A key step for the recovery and reutilization of the surfactants is the removal of the thiocarbonothioylthio end-group, which prevents the chemical grafting of the surfactant in the growing polymer chains. This is also useful to avoid the polymer contamination with the surfactant, which could affect the final thermo-mechanical properties of the material.

■ ASSOCIATED CONTENT

Supporting Information

The Supporting Information is available free of charge at <https://pubs.acs.org/doi/10.1021/acsapm.1c01266>.

¹H NMR spectra of the thermo-responsive surfactants, size and PDI of the surfactant micelles, of the same micelles after the elimination of the RAFT agent with AIBN, and of the NPs obtained through the eFRP of

MMA, BMA, and STY using the thermo-responsive surfactants as stabilizers, and stability of the surfactant micelles at different pH (PDF)

AUTHOR INFORMATION

Corresponding Author

Mattia Sponchioni – Department of Chemistry, Materials and Chemical Engineering “Giulio Natta”, Politecnico di Milano, 2013 Milano, Italy; orcid.org/0000-0002-8130-6495; Email: mattia.sponchioni@polimi.it

Authors

Nicolò Manfredini – Department of Chemistry, Materials and Chemical Engineering “Giulio Natta”, Politecnico di Milano, 2013 Milano, Italy

Daive Moscatelli – Department of Chemistry, Materials and Chemical Engineering “Giulio Natta”, Politecnico di Milano, 2013 Milano, Italy; orcid.org/0000-0003-2759-9781

Complete contact information is available at:
<https://pubs.acs.org/10.1021/acsapm.1c01266>

Notes

The authors declare no competing financial interest.

ACKNOWLEDGMENTS

The authors are grateful to Sergio Del Grande and Giulia Lentoni for the help with the measurement of the CMC and Roberto Panebianco for the help with the DLS analysis.

REFERENCES

- (1) Hopewell, J.; Dvorak, R.; Kosior, E. Plastics Recycling: Challenges and Opportunities. *Philos. Trans. R. Soc., B* **2009**, *364*, 2115–2126.
- (2) Thompson, R. C.; Moore, C. J.; vom Saal, F. S.; Swan, S. H. Plastics, the Environment and Human Health: Current Consensus and Future Trends. *Philos. Trans. R. Soc., B* **2009**, *364*, 2153–2166.
- (3) Plastics Europe—Association of Plastic Manufacturers (Organization). *Plastics—The Facts 2020*; PlasticEurope, 2020; Vol 16, pp 1–64.
- (4) Liang, X.-M.; Jiang, H.-C.; Fang, J.-L.; Hua, M.; Pan, X.-H.; Jiang, J.-C. Thermal Analysis of the Styrene Bulk Polymerization and Characterization of Polystyrene Initiated by Two Methods. *Chem. Eng. Commun.* **2019**, *206*, 432–443.
- (5) Asua, J. M. *Polymer Dispersions: Principles and Applications*; Springer: Netherlands, 1997.
- (6) Liu, Y.; Jessop, P. G.; Cunningham, M.; Eckert, C. A.; Liotta, C. L. Switchable Surfactants. *Science* **2006**, *313*, 958–960.
- (7) Wang, F.; Luo, Y.; Li, B.-G.; Zhu, S. Synthesis and Redispersibility of Poly(styrene-block-n-butyl acrylate) Core-Shell Latexes by Emulsion Polymerization with RAFT Agent-Surfactant Design. *Macromolecules* **2015**, *48*, 1313–1319.
- (8) Zhang, Q.; Yu, G.; Wang, W.-J.; Yuan, H.; Li, B.-G.; Zhu, S. Switchable Block Copolymer Surfactants for Preparation of Reversibly Coagulatable and Redispersible Poly(Methyl Methacrylate) Latexes. *Macromolecules* **2013**, *46*, 1261–1267.
- (9) Li, Y.; Liu, L.; Liu, X.; Chen, S.; Fang, Y. Reversibly Responsive Microemulsion Triggered by Redox Reactions. *J. Colloid Interface Sci.* **2019**, *540*, 51–58.
- (10) Jessop, P. G.; Mercer, S. M.; Heldebrant, D. J. CO₂-Triggered Switchable Solvents, Surfactants, and Other Materials. *Energy Environ. Sci.* **2012**, *5*, 7240–7253.
- (11) Liu, P.; Lu, W.; Wang, W.-J.; Li, B.-G.; Zhu, S. Highly CO₂/N₂-Switchable Zwitterionic Surfactant for Pickering Emulsions at Ambient Temperature. *Langmuir* **2014**, *30*, 10248–10255.
- (12) Chen, W.; He, H.; Zhu, H.; Cheng, M.; Li, Y.; Wang, S. Thermo-Responsive Cellulose-Based Material with Switchable Wettability for Controllable Oil/Water Separation. *Polymers* **2018**, *10*, 592.
- (13) Li, J.-J.; Zhu, L.-T.; Luo, Z.-H. Electrospun Fibrous Membrane with Enhanced Switchable Oil/Water Wettability for Oily Water Separation. *Chem. Eng. J.* **2016**, *287*, 474–481.
- (14) Yuan, X.; Li, W.; Zhu, Z.; Han, N.; Zhang, X. Thermo-Responsive PVDF/PSMA Composite Membranes with Micro/Nanoscale Hierarchical Structures for Oil/Water Emulsion Separation. *Colloids Surf., A* **2017**, *516*, 305–316.
- (15) Lee, M. F. X.; Chan, E. S.; Tam, K. C.; Tey, B. T. Thermo-Responsive Adsorbent for Size-Selective Protein Adsorption. *J. Chromatogr. A* **2015**, *1394*, 71–80.
- (16) Mizutani, A.; Nagase, K.; Kikuchi, A.; Kanazawa, H.; Akiyama, Y.; Kobayashi, J.; Annaka, M.; Okano, T. Thermo-Responsive Polymer Brush-Grafted Porous Polystyrene Beads for All-Aqueous Chromatography. *J. Chromatogr. A* **2010**, *1217*, 522–529.
- (17) Bauer, J.; Verbunt, P. P. C.; Lin, W.-Y.; Han, Y.; Van, M.-P.; Cornelissen, H. J.; Yu, J. J. H.; Bastiaansen, C. W. M.; Broer, D. J. Thermoresponsive Scattering Coating for Smart White LEDs. *Opt. Express* **2014**, *22*, A1868.
- (18) Fei, X.; Lu, T.; Ma, J.; Zhu, S.; Zhang, D. A Bioinspired Poly(N-Isopropylacrylamide)/Silver Nanocomposite as a Photonic Crystal with Both Optical and Thermal Responses. *Nanoscale* **2017**, *9*, 12969–12975.
- (19) Sponchioni, M.; Ferrari, R.; Morosi, L.; Moscatelli, D. Influence of the Polymer Structure over Self-Assembly and Thermo-Responsive Properties: The Case of PEG-b-PCL Grafted Copolymers via a Combination of RAFT and ROP. *J. Polym. Sci., Part A: Polym. Chem.* **2016**, *54*, 2919–2931.
- (20) Pan, G.; Guo, Q.; Cao, C.; Yang, H.; Li, B. Thermo-Responsive Molecularly Imprinted Nanogels for Specific Recognition and Controlled Release of Proteins. *Soft Matter* **2013**, *9*, 3840–3850.
- (21) Sponchioni, M.; Rodrigues Bassam, P.; Moscatelli, D.; Arosio, P.; Capasso Palmiero, U. Biodegradable Zwitterionic Nanoparticles with Tunable UCST-Type Phase Separation under Physiological Conditions. *Nanoscale* **2019**, *11*, 16582–16591.
- (22) Sponchioni, M.; O'Brien, C. T.; Borchers, C.; Wang, E.; Rivolta, M. N.; Penfold, N. J. W.; Canton, I.; Armes, S. P. Probing the Mechanism for Hydrogel-Based Stasis Induction in Human Pluripotent Stem Cells: Is the Chemical Functionality of the Hydrogel Important? *Chem. Sci.* **2020**, *11*, 232–240.
- (23) Sponchioni, M.; Capasso Palmiero, U.; Manfredini, N.; Moscatelli, D. RAFT Copolymerization of Oppositely Charged Monomers and Its Use to Tailor the Composition of Nonfouling Polyampholytes with an UCST Behaviour. *React. Chem. Eng.* **2019**, *4*, 436–446.
- (24) Sponchioni, M.; Capasso Palmiero, U.; Moscatelli, D. Thermo-Responsive Polymers: Applications of Smart Materials in Drug Delivery and Tissue Engineering. *Mater. Sci. Eng., C* **2019**, *102*, 589–605.
- (25) Halperin, A.; Kröger, M.; Winnik, F. M. Poly(N-Isopropylacrylamide) Phase Diagrams: Fifty Years of Research. *Angew. Chem., Int. Ed.* **2015**, *54*, 15342–15367.
- (26) Zhang, Q.; Weber, C.; Schubert, U. S.; Hoogenboom, R. Thermoresponsive Polymers with Lower Critical Solution Temperature: From Fundamental Aspects and Measuring Techniques to Recommended Turbidimetry Conditions. *Mater. Horiz.* **2017**, *4*, 109–116.
- (27) Niskanen, J.; Tenhu, H. How to Manipulate the Upper Critical Solution Temperature (UCST)? *Polym. Chem.* **2017**, *8*, 220–232.
- (28) Seuring, J.; Agarwal, S. Polymers with Upper Critical Solution Temperature in Aqueous Solution: Unexpected Properties from Known Building Blocks. *ACS Macro Lett.* **2013**, *2*, 597–600.
- (29) Manfredini, N.; Tomasoni, M.; Sponchioni, M.; Moscatelli, D. Influence of the Polymer Microstructure over the Phase Separation of Thermo-Responsive Nanoparticles. *Polymers* **2021**, *13*, 1032.
- (30) Griffin, W. C. Classification of Surface-Active Agents by “HLB”. *J. Soc. Cosmet. Chem.* **1949**, *1*, 311–326.

(31) Manfredini, N.; Ilare, J.; Invernizzi, M.; Polvara, E.; Contreras Mejia, D.; Sironi, S.; Moscatelli, D.; Sponchioni, M. Polymer Nanoparticles for the Release of Fragrances: How the Physicochemical Properties Influence the Adsorption on Textile and the Delivery of Limonene. *Ind. Eng. Chem. Res.* **2020**, *59*, 12766–12773.

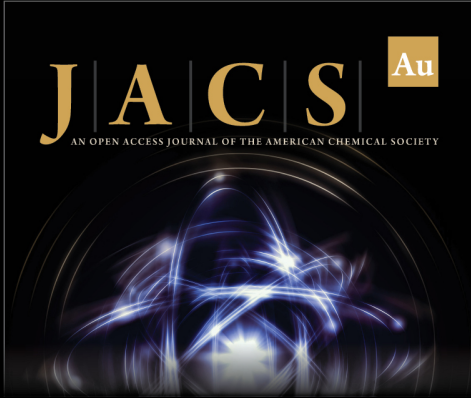
(32) Gaynanova, G. A.; Vagapova, G. I.; Valeeva, F. G.; Vasilieva, E. A.; Galkina, I. V.; Zakharova, L. Y.; Sinyashin, O. G. A Novel Supramolecular Catalytic System Based on Amphiphilic Triphenylphosphonium Bromide for the Hydrolysis of Phosphorus Acid Esters. *Colloids Surf., A* **2016**, *489*, 95–102.

(33) Lutz, J.-F. Polymerization of Oligo(Ethylene Glycol) (Meth)Acrylates: Toward New Generations of Smart Biocompatible Materials. *J. Polym. Sci., Part A: Polym. Chem.* **2008**, *46*, 3459–3470.


(34) Capasso Palmiero, U.; Sponchioni, M.; Manfredini, N.; Maraldi, M.; Moscatelli, D. Strategies to Combine ROP with ATRP or RAFT Polymerization for the Synthesis of Biodegradable Polymeric Nanoparticles for Biomedical Applications. *Polym. Chem.* **2018**, *9*, 4084–4099.


(35) Palmiero, U. C.; Agostini, A.; Gatti, S.; Sponchioni, M.; Valenti, V.; Brunel, L.; Moscatelli, D. RAFT Macro-Surfmers and Their Use in the Ab Initio RAFT Emulsion Polymerization To Decouple Nanoparticle Size and Polymer Molecular Weight. *Macromolecules* **2016**, *49*, 8387–8396.


(36) Motin, M. A.; Hafiz Mia, M. A.; Nasimul Islam, A. K. M. Thermodynamic Properties of Sodium Dodecyl Sulfate Aqueous Solutions with Methanol, Ethanol, n-Propanol and Iso-Propanol at Different Temperatures. *J. Saudi Chem. Soc.* **2015**, *19*, 172–180.



JACS Au
AN OPEN ACCESS JOURNAL OF THE AMERICAN CHEMICAL SOCIETY

 Editor-in-Chief
Prof. Christopher W. Jones
Georgia Institute of Technology, USA

Open for Submissions 

pubs.acs.org/jacsau  ACS Publications
Most Trusted. Most Cited. Most Read.